

Power Stabilization of Dynamic Wireless Power Transfer System with Grid-connected Photovoltaic and DC Bus Voltage Control

Nozomi MURAYAMA
Faculty of Science and Technology
Tokyo University of Science
Noda, Japan
murayama.nozomi23@gmail.com

Takehiro IMURA
Faculty of Science and Technology
Tokyo University of Science
Noda, Japan

Yoichi HORI
Faculty of Science and Technology
Tokyo University of Science
Noda, Japan

Abstract— Dynamic Wireless Power Transfer (DWPT), which has been attracting attention in recent years, is a system that solves the problems of Electric Vehicles (EVs), such as long charging times and short cruising ranges. This study proposes a system for local production and local consumption of electricity by using grid-connected photovoltaic (PV) as an energy source for DWPT. When the PV is generating excess power compared to the electricity demand, the power is returned to the grid. When the PV is not generating enough power, the grid subsidizes the shortage. In this way, the DCbus voltage can be maintained at a constant level, enabling a stable supply of power to the EV on the demand side. The effectiveness of the proposed system was verified using circuit analysis software (MATLAB/Simulink), which enables stable DWPT while performing maximum power point tracking (MPPT) control of the PV panels and DCbus voltage control using a Dual Active Bridge (DAB) converter connected to the Grid side. The results show that the DCbus voltage can be controlled within plus or minus 1 percent of the target value regardless of the fluctuating PV and the coupling coefficient between the transmission and receiving coils, and the power conversion efficiency of the DWPT was up to 70 percent. Thus, the proposed system was found to be effective and feasible.

Keywords—Dynamic Wireless Power Transfer, Photovoltaic, Electric Vehicles, MPPT, Grid-connected, DAB converter, DC bus

I. INTRODUCTION

In recent years, there has been a strong global trend toward decarbonization, which calls for a shift from gasoline-powered vehicles that emit CO₂ to electric vehicles that are powered by electricity. However, several issues remain with EVs. First, the cruising range is shorter than that of gasoline-powered vehicles. This is largely related to the on-board battery. Simply increasing battery capacity is not a desirable solution because it will lead to a price increase for the vehicle itself. In addition, the lack of charging facilities and the long time required to charge them have also hindered the spread of EVs. As a solution to these issues, Dynamic Wireless Power Transfer (DWPT), which wirelessly transmits electric power

from roadside facilities to a moving EV, has been studied [1]-[4].

DWPT systems can also improve the charging infrastructure and increase range without enlarging the battery capacity. Furthermore, the use of photovoltaic (PV), a renewable energy source, as the power source for DWPT will lead to further decarbonization. This paper proposes a PV + DWPT system in which the power source of the DWPT is grid-connected solar power. Several studies of systems combining PV and DWPT exist [5]-[10]. In [6], PV is installed on top of an EV, and in addition to DWPT, the PV power is sent directly to the battery. In [7], [8], and [9], when off-grid PV generates excess electricity, it is stored in a battery, from which power is supplied when the PV is not generating. In [10], PV is connected to the grid, but the grid and DCbus are not isolated, making the system impractical. In [5], which is the focus of this study, PV and Grid are swapped using a switch, which means that PV generation is stopped when DWPT is not performed. To eliminate this waste of power, this paper installs a Dual Active Bridge (DAB) converter. This isolated bidirectional DC/DC converter returns PV power to the DC grid when PV is generating excess power and compensates for the power shortage from the grid when PV power is insufficient. Furthermore, a DAB converter is used to control the DCbus voltage to enable stable DWPT. The effectiveness of the proposed system is verified using circuit analysis software. In section II, the overall system of the proposed PV+Grid+DWPT system is presented. In section III, the simulation details of the proposed system are shown. Finally, IV presents the conclusion.

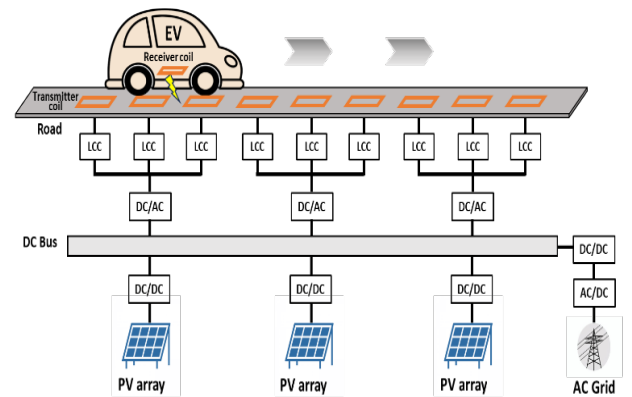


Fig.1 Overall picture of grid-connected PV+DWPT system

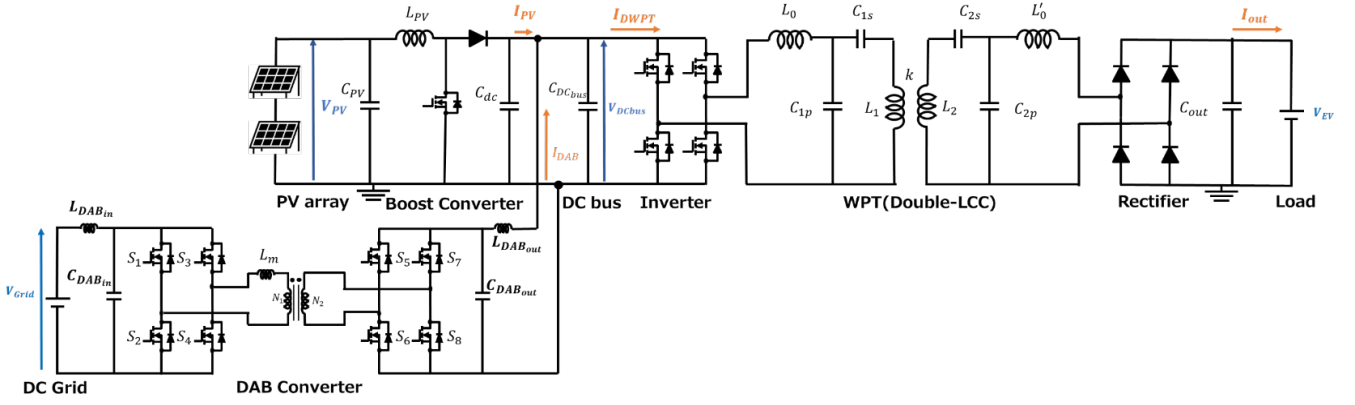


Fig.2 Schematic diagram of proposed system

II. PROPOSED PV+DWPT SYSTEM

An overall picture of the proposed system is shown in Fig. 1. As shown in Fig. 1, the PV and AC Grid are connected to a common DC Bus, each through a converter. The PV and AC Grid are then connected to a power transmission coil buried in the road. When the EV drives on the road, the power is sent from the transmission coil to the receiving coil mounted on the EV by magnetic field coupling, and the battery is charged via the DC/DC converter. Fig. 2 shows the schematic diagram of the proposed system. From Fig. 2, many PV panels are installed near the road where power is supplied, and MPPT control is performed by a DC/DC boost converter operating at a switching frequency of 10 kHz so that maximum PV power is always available. As mentioned in the introduction of I, the power grid is connected to stabilize the fluctuating PV power. In this paper, however, the AC grid and AC/DC converter are treated as a simplified DC grid. The DC grid is connected to a DAB converter, and the switching frequency of the DAB converter operates at 50 kHz square wave. By controlling the output current of the DAB converter, the DCbus is operated at a constant voltage. The DC/AC inverter after the DCbus is operated at a switching frequency of 85 kHz. Finally, an LCC topology, in which an LCL filter with gyrator characteristics is applied to the wireless power transmission (WPT) topology, is used to send power from the transmitter coil (road side) to the receiver coil (vehicle side) to charge the EV's battery. This study simplifies the EV side DC/DC boost converter and battery voltage to a constant voltage source.

A. Double-LCC Topology Used in DWPT

The basic circuit of the DWPT system studied in this paper is shown in Fig. 3. The reason for using the Double-LCC method among various magnetic resonance coupling methods is that when the coupling coefficient k is 0, no current flows in the transmitter coil due to the input impedance characteristic of the primary side. This characteristic eliminates the need for vehicle detection on the receiving side and ON/OFF control on the transmission side. In Fig. 3, the LCC circuit is designed so that LC resonance occurs in each closed circuit, and the resonance conditions are shown in equations (1) and (2) below.

$$\text{Transmission side : } f_0 = \frac{1}{2\pi\sqrt{L_0C_{1p}}} = \frac{1}{2\pi\sqrt{\frac{C_{1p} + C_{1s}}{L_1C_{1p}C_{1s}}}} \quad (1)$$

$$\text{Receiving side : } f_0 = \frac{1}{2\pi\sqrt{L'_0C_{2p}}} = \frac{1}{2\pi\sqrt{\frac{C_{2p} + C_{2s}}{L_2C_{2p}C_{2s}}}} \quad (2)$$

B. DAB Converter

DAB converters are frequently used as isolated bidirectional DC/DC converters for transforming high voltages in power systems and for bidirectional power transmission [11]-[13]. The reason for this is that they enable zero-voltage switching while maintaining high density and also have high power transmission efficiency. Therefore, in this paper, a DAB converter is connected to the DCgrid to achieve constant DCbus voltage. The basic circuit of the DAB converter is shown in Fig. 4. The DAB converter consists of two full-bridge circuits connected to a high-frequency transformer, which isolates the primary (left side) and secondary (right side) full-bridge circuits. The primary full-bridge circuit is connected to the DCgrid and the secondary to the DCbus. Bidirectional power transmission can be maintained or controlled by changing the phase angle of the secondary side relative to the primary side.

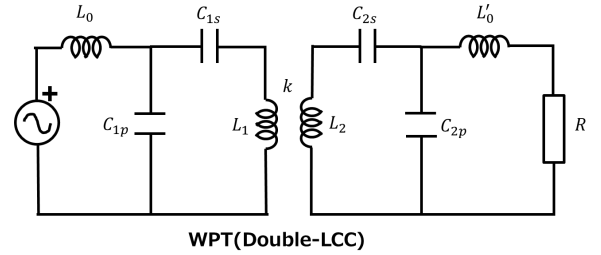


Fig.3 Basic circuit of Double-LCC topology

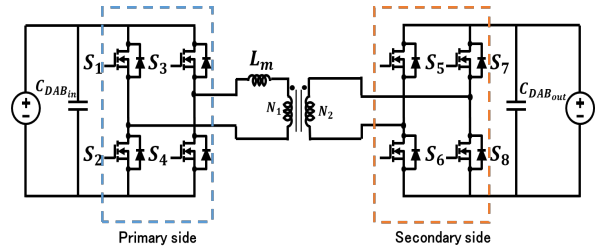


Fig.4 Basic circuit of DAB converter

C. Control Method of DAB Converter

Constant voltage control of the DCbus is performed by phase shifting the DAB converter. Referring to [11], Fig. 5 shows the control block diagram of the DAB converter.

The target voltage value of the DC bus; $V_{DCbusref}$ is compared with the measured value; V_{DCbus} , and PI control is performed to obtain I_{fb} . Next, feed-forward control is performed from the measured value I_{DAB} to obtain I_{ff} . Then, using the target value of the output current I_{DABref} obtained by adding I_{fb} and I_{ff} together, the phase angle φ of the secondary side is determined and the phase shift is performed.

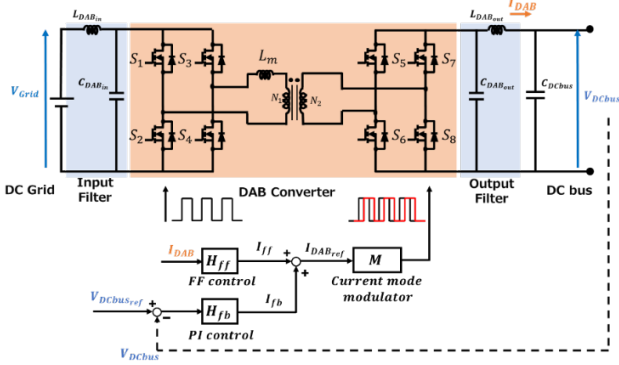


Fig.5 Block diagram of DAB converter control

Table.1 Simulation Parameters

(a) PV parameters

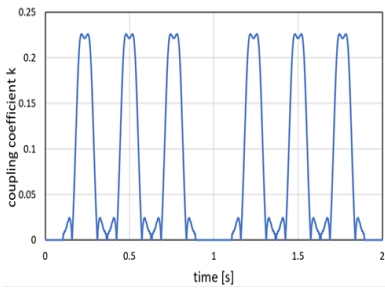
$f_{PV}[kHz]$	Δd	Duty sample	$L_{PV}[mH]$	$C_{PV}[\mu F]$	$C_{dc}[\mu F]$
10	0.01	0.01	0.1	500	100

(b) DAB parameters

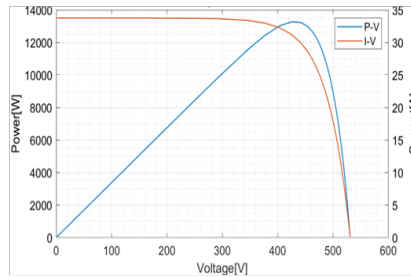
$f_{DAB}[kHz]$	$V_{grid}[V]$	$V_{DCbusref}[V]$	n_t	$L_m[\mu H]$	$C_{DCbus}[\mu F]$
50	2400	600	4	50	500

(c) DWPT parameters

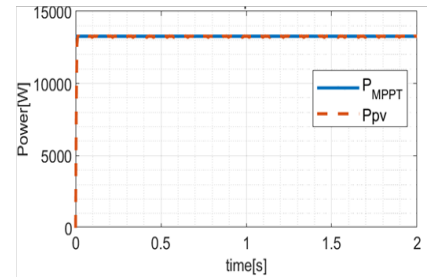
$f_{INV}[kHz]$	$L_0[\mu H]$	$C_{1p}[nF]$	$C_{1s}[nF]$	$L_1[\mu H]$	$L'_0[\mu H]$	$C_{2p}[nF]$	$C_{2s}[nF]$	$L_2[\mu H]$
85	54	65	23	207	49	71	56	111



(a) Coupling coefficient k

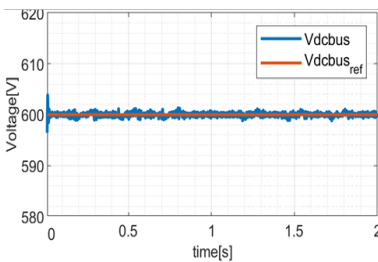


(b) P-V, I-V curve

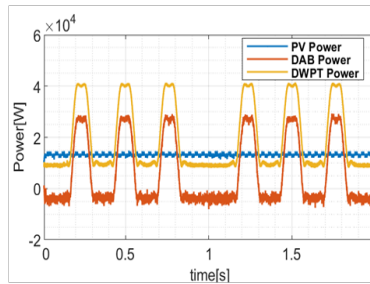


(c) P_{PV} tracking P_{MPP}

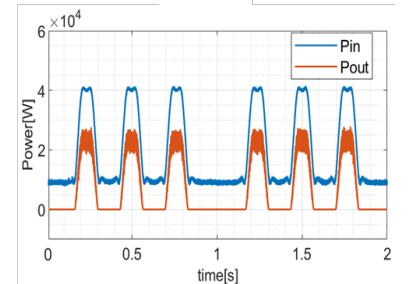
Fig.6 Coupling coefficient transition, P-V and I-V curve, results of MPPT.



(a) V_{DCbus} against $V_{DCbusref}$



(b) Power of PV, DAB, DWPT



(c) Input&output power of DWPT

Fig.7 Results of DAB current and power of PV, DAB, DWPT.

In this way, power adjustment of the DCgrid is made possible. The following formula (3) shows how to obtain the phase angle φ . Here, the direction sent from DCgrid to DCbus is the positive direction of I_{DABref} .

$$\varphi = \begin{cases} \frac{\pi}{2} - \frac{\pi}{2} \sqrt{1 - \left(\frac{8f_{DAB}L_mI_{DABref}}{n_tV_{grid}} \right)^2} & (I_{DABref} > 0) \\ -\frac{\pi}{2} + \frac{\pi}{2} \sqrt{1 - \left(\frac{8f_{DAB}L_mI_{DABref}}{n_tV_{grid}} \right)^2} & (I_{DABref} < 0) \end{cases} \quad (3)$$

III. SIMULATION METHODS AND RESULTS

A. Simulation Methods

Simulation of the proposed system is performed using circuit analysis software based on the circuit diagram in Fig. 2. The coupling coefficient k is set so that an EV with one receiving coil between 0-2 seconds runs over a transmission coil with a 50% laying ratio. This paper presents through simulation that the DCbus voltage remains constant and stable DWPT is performed regardless of the variation of the coupling coefficient between the transmitter and receiver coils.

The parameters used in the simulation are shown in Table 1. In (a), the PV panel parameters are shown: the switching frequency of the DC/DC converter is set as f_{PV} , the minute variation amount when the duty ratio is changed by MPPT using the mountain-climbing method is set as Δd and the sampling time to update the duty ratio is set as $duty\ sample$. In (b), the parameters around the DAB converter are shown. The switching frequency of the DAB converter is set as f_{DAB} , the turn ratio of the transformer is set as n_t , and the value of DC grid and the target value of DCbus voltage is V_{grid} and $V_{DCbusref}$, respectively. In (c), the parameters of DWPT are shown. The switching frequency of the inverter is set as f_{INV} and the value of the resonant elements of the Double-LCC circuit are shown. In (4)-(7), the formulas for calculating power for each parameter are shown.

$$P_{PV} = V_{PV} * I_{PV} \quad (4)$$

$$P_{grid} = V_{DCbus} * I_{DAB} \quad (5)$$

$$P_{in} = V_{DCbus} * I_{DWPT} \quad (6)$$

$$P_{out} = V_{out} * I_{out} \quad (7)$$

P_{PV} represents the output power of PV, and P_{grid} represents the amount of power when the direction in which power is sent from DCgrid to DCbus is the positive direction of I_{DAB} . P_{in} represents the input power of DWPT, and P_{out} represents the output power of DWPT.

B. Simulation Results and Discussion

Simulation results are shown in Figs. 6 and 7. Fig. 6 shows the coupling coefficient of the DWPT and the results around the PV. (a) shows the variation of the coupling coefficient from 0-2 seconds, and (b) shows the amount of power generated from an irradiance of 1000 W/m² at the PV panels, showing that as the voltage changes, the amount of power generated also changes, with the maximum power around 13 kW. In (c), P_{PV} tracks P_{MPPT} , indicating that the MPPT control is working properly.

Fig. 7 shows the results around the DAB converter and DWPT. In (a), the DCbus voltage variation is shown. When $V_{DCbusref}$ is set to 600V, V_{DCbus} is kept constant within $\pm 1\%$ of the target value. Therefore, it can be said that the constant voltage control was successfully performed. In (b), the variations of P_{PV} , P_{Grid} ($= P_{DAB}$), and P_{DWPT} are shown. The results show that when there is no demand on the DWPT side, the PV power returns to the DC grid. Also, when the EV runs on the six transmitter coils, the DC grid supplies the power that is not enough for the PV alone. This indicates that the DC grid absorbs and sends out power according to the power fluctuations of the PV and DWPT. Therefore, it can be said that DWPT is stably operated without wasting the power generated by PV. In (c), P_{in} and P_{out} are shown. From the results, power was sent to the vehicle side due to the variation of the coupling coefficient between the transmitter and receiver coils, and the power transmission efficiency was about 70% at maximum. One possible reason for the relatively low power transmission efficiency is that the circuit on the EV side is simplified to a constant voltage source. Also, standby power is seen when the EV is not running on the transmitter coil, but this may be because the connected inverter does not perform switching control to reduce standby loss.

IV. CONCLUSION

In this paper, we proposed a grid-connected PV+DWPT system and demonstrated the system through simulations. The simulation results show that the MPPT control of the PV was successfully performed while DWPT was used. Furthermore, the connected power system was able to absorb or supply the excess or shortage of PV and keep the DCbus voltage constant within $\pm 1\%$ of the target value. thus enabling a stable DWPT of 70% power transmission efficiency. Based on the simulation results, the proposed grid-connected PV+DWPT system has proven to be a feasible system that enables local production and local consumption of electricity.

As a future effort, we are working on bench-scale experiments and plan to further verify the effectiveness of the proposed system. In addition, we will examine how the constant voltage control works when PV fluctuates significantly, and work to increase the power transmission efficiency and reduce standby losses.

REFERENCES

- [1] A. C. Bagchi, A. Kamineni, R. A. Zane and R. Carlson, "Review and Comparative Analysis of Topologies and Control Methods in Dynamic Wireless Charging of Electric Vehicles," in *IEEE Journal of Emerging and Selected Topics in Power Electronics*, vol. 9, no. 4, pp. 4947-4962, Aug. 2021.
- [2] R. Tavakoli, T. Shabanian, E. M. Dede, C. Chou and Z. Pantic, "EV Misalignment Estimation in DWPT Systems Utilizing the Roadside Charging Pads," in *IEEE Transactions on Transportation Electrification*, vol. 8, no. 1, pp. 752-766, March 2022.
- [3] A. N. Azad, A. Echols, V. A. Kulyukin, R. Zane and Z. Pantic, "Analysis, Optimization, and Demonstration of a Vehicular Detection System Intended for Dynamic Wireless Charging Applications," in *IEEE Transactions on Transportation Electrification*, vol. 5, no. 1, pp. 147-161, March 2019.
- [4] R. Tavakoli and Z. Pantic, "Analysis, Design, and Demonstration of a 25- kW Dynamic Wireless Charging System for Roadway Electric Vehicles," in *IEEE Journal of Emerging and Selected Topics in Power Electronics*, vol. 6, no. 3, pp. 1378-1393, Sept. 2018.
- [5] K. Kumar, K. V. V. S. R. Chowdary, P. Sanjeevikumar and R. Prasad, "Analysis of Solar PV Fed Dynamic Wireless Charging System for Electric Vehicles," *IECON 2021 – 47th Annual Conference of the IEEE Industrial Electronics Society*, Toronto, ON, Canada, 2021, pp. 1-6.
- [6] P. S. R. Nayak, K. Kamalpathi, N. Laxman and V. K. Tyagi, "Design and Simulation Of BUCK-BOOST Type Dual Input DC-DC Converter for Battery Charging Application in Electric Vehicle," 2021 International Conference on Sustainable Energy and Future Electric Transportation (SEFET), 2021, pp. 1-6.
- [7] A. Babaki, S. Vaez-Zadeh, M. F. Moghaddam and A. Zakerian, "A Novel Multi-Objective Topology for In-Motion WPT Systems with an Input DG Source," 2019 10th International Power Electronics, Drive Systems and Technologies Conference (PEDSTC), 2019, pp. 787-792.
- [8] T. M. Newbolt, P. Mandal, H. Wang and R. Zane, "Diverse Effects of Dynamic Wireless Power Transfer Roadway In-Motion Electric Vehicle Charging," *2023 IEEE Power & Energy Society Innovative Smart Grid Technologies Conference (ISGT)*, Washington, DC, USA, 2023, pp. 1-5.
- [9] M. Sugizaki, S. Urano, T. Imura and Y. Hori, "Proposal for the System of Dynamic Wireless Power Transfer Connected with Photovoltaic in the Off-Grid Environment," *2022 IEEE 7th Southern Power Electronics Conference (SPEC)*, Nadi, Fiji, 2022, pp. 1-6.
- [10] S. Urano, M. Sugizaki, T. Imura and Y. Hori, "Basic Experiment on the Integration of Grid-Connected Photovoltaic and Dynamic Wireless Power Transfer," *2022 IEEE 7th Southern Power Electronics Conference (SPEC)*, Nadi, Fiji, 2022, pp. 1-6.
- [11] Z. Shan, J. Jatskevich, H. H. -C. Lu and T. Fernando, "Simplified Load-Feedforward Control Design for Dual-Active-Bridge Converters With Current-Mode Modulation," in *IEEE Journal of Emerging and Selected Topics in Power Electronics*, vol. 6, no. 4, pp. 2073-2085, Dec. 2018.
- [12] P. Pal and R. K. Behera, "Observer Based Current Sensorless Control for DAB Converter with Improved Dynamic Performance," *2022 IEEE International Conference on Power Electronics, Drives and Energy Systems (PEDES)*, Jaipur, India, 2022, pp. 1-6.
- [13] Y. -C. Jeung and D. -C. Lee, "Sliding mode control of bi-directional dual active bridge DC/DC converters for battery energy storage systems," *2017 IEEE Applied Power Electronics Conference and Exposition (APEC)*, Tampa, FL, USA, 2017.